Carbohydrate Polymers 114 (2014) 330–338

Contents lists available at ScienceDirect

Carbohydrate Polymers

journal homepage: www.elsevier.com/locate/carbpol

Fabrication of thermoplastic ductile films of chitin butyrate/poly(ε-caprolactone) blends and their cytocompatibility

Hiroki Hashiwaki[a], Yoshikuni Teramoto[b,*], Yoshiyuki Nishio[a]

[a] Division of Forest and Biomaterials Science, Graduate School of Agriculture, Kyoto University, Kitashirakawa Oiwake-cho, Sakyo-ku, Kyoto 606-8502, Japan
[b] Course of Applied Life Science, Faculty of Applied Biological Sciences, Gifu University, 1-1 Yanagido, Gifu 501-1193, Japan

ARTICLE INFO

Article history:
Received 17 June 2014
Received in revised form 18 August 2014
Accepted 18 August 2014
Available online 24 August 2014

Keywords:
Chitin butyrate
Poly(ε-caprolactone)
Blend
Tensile property
Cytocompatibility

ABSTRACT

We fabricate thermoplastic films of chitin burtyrate (ChB)/poly(ε-caprolactone) (PCL) blends with different degree of miscibility (miscible (M), partially miscible (PM), and immiscible (IM)), and examined the feasibility as a cell scaffold system through evaluating mechanical properties and cytocompatibility. We found a remediation of the brittleness and an increase in ductility of ChB by blending PCL for the M and PM blends. The blend films were subjected to alkaline hydrolysis (2-M NaOH/37 °C/48 h) with expectation of the improvement of the surface hydrophilicity and cell accessibility. ATR-FTIR spectroscopy of the alkaline-treated PM and IM films revealed that PCL component and ester side-chains of acyl chitin were selectively removed from the surface domain. L929 fibroblast cells well adhered and proliferated on these films. Therefore, the materials possess a great potential for the utilization as a thermoplastic cell scaffold in tissue engineering by adequate selection of the degree of miscibility and post treatment.

1. Introduction

Chitin has a large potential for developing specially functionalized materials in medical and sanitary fields, because of its excellent biological properties such as biodegradability, biocompatibility, and antibacterial and wound healing activity. Despite its promising potential, the major imperfections of chitin are poor thermal processability and less film ductility albeit its stiffness, which limit its application in tissue engineering (Jayakumar, Prabaharan, Nair, & Tamura, 2010; Khor & Lim, 2003; Muzzarelli, 2009). Meanwhile, poly(ε-caprolactone) (PCL), approved as biodegradable and biocompatible polyester, has high ductility, but its poor hydrophilicity, slow degradation kinetics, and no natural cell recognition sites greatly restrict its application in the biomedical field (Prabhakaran et al., 2008). Various kinds of physicochemical and surface modification techniques have been used to overcome these shortcomings (Dubas, Kittitheeranun, Rangkupan, Sanchavanakit, & Potiyaraj, 2009; He et al., 2012; Jeong et al., 2008; Zhu, Gao, Liu, & Shen, 2002). Even though PCL has attracted interest as a blending partner of chitinous (Chen, Sun, & Ren, 2005; Honma, Senda, & Inoue, 2003; Sarasam & Madihally, 2005; Senda, He, & Inoue, 2002; Wan, Wu, Cao, & Dalai, 2008) to obtain more advanced biocompatible materials by complementing each other's contradictory features, it seems to have been difficult to obtain their physically tough intimate mixtures on the nanoscopic scale.

Recently, we have successfully attained a series of thermodynamically miscible blends of such a combination (Sugimoto, Kawahara, Teramoto, & Nishio, 2010). Namely, we prepared solvent-soluble acyl chitin derivatives having a normal acyl group and investigated effects of the side-chain length (side-chain carbon number, *N*; 2–6) and the degree of substitution (DS) on the miscibility of solution cast blends with PCL. NMR analysis quantitatively demonstrated the acylations not only for C3/C6 hydroxyl protons but also for C2 amino proton(s), where amide-DS for the *N*-acylation and ester-DS for the *O*-acylation were determined as the average numbers of acyl substitution associated with C2-NHCOR/C2-NH_2 and C3-OH/C6-OH, respectively, per glucosamine residue of chitin. It was revealed that the acetate ($N = 2$) was immiscible with PCL even in the highly acetylated state of total-DS (=amide-DS + ester-DS) = 3.8, while other acyl chitin products ($N = 3$–6) showed miscibility with PCL when totally high-substituted grades of them (total-DS ≥ 3) were used. The degree of miscibility was enhanced definitely with an increase in ester-DS, but it made less correlation with amide-DS. Fig. S1 summarizes the result of the miscibility estimation, clearly indicating that the degree of miscibility was adaptable by *N* as well as by DS.

* Corresponding author. Tel.: +81 58 293 2917.
E-mail address: teramoto@gifu-u.ac.jp (Y. Teramoto).

http://dx.doi.org/10.1016/j.carbpol.2014.08.028
0144-8617/

In the present study, we examined the feasibility of using chitin butyrate (ChB, $N = 4$)/PCL (50/50 in weight) based films prepared by hot-pressing as a thermoplastic flexible cell scaffold system. The chitin derivative ChB has recently been evaluated for biomedical applications using its fibrous forms prepared via a dissolution-regeneration process (Draczynski, Bogun, Mikolajczyk, Szparaga, & Krol, 2013; Muzzarelli et al., 2005; Pant et al., 2013). Contrastively, in this study, the thermoplasticity was introduced to the chitinous component by intimately combining PCL as an external plasticizer, potentially providing the scaffold of varied three-dimensional forms. We investigated how the blend miscibility influences the tensile mechanical property of the thermally molded films. Actually, however, mechanical properties of blend systems are sometimes deteriorated for the combinations of high degree of miscibility. Meanwhile, in general, the film toughness and ductility can be accomplished by high dispersion of microcrystallite and introduction of cross-linkages. Therefore, we will discuss the mechanical performance of the blend films in connection not only with miscibility but also with the crystallinity of the PCL component and scale of homogeneity of the blend components. Subsequently, we performed an alkaline treatment (2-M NaOH at 37 °C for 48 h) for the thermally molded blend films, expecting the improvement of the surface hydrophilicity and accessibility for cells because of a possible enrichment of the surface with bioactive chitinous compound. We characterized surface morphology and chemical compositions of the alkaline-treated films and explored the cytocompatiblility of mouse fibroblast cells (L929) using the blend films.

2. Experimental

2.1. Materials

As our preceding paper (Sugimoto et al., 2010), an original material of chitin isolated from crab shells (Fluka 22720 Chitin Lot & Filling code: 405226/1 12900) was according to a Hackman's method (Hackman, 1954). The nominal molecular weight of the chitin material is 400,000 and the viscosity average degree of polymerization (DP) was determined to be 380 (Sugimoto et al., 2010). The degree of deacetylation (DD) of the purified chitin was 5.0%, determined by infrared spectroscopy (Sannan, Kurita, Ogura, & Iwakura, 1978). PCL with a nominal weight-average molecular weight of 70,000–100,000 was purchased from Wako Pure Chemical Industries, Ltd., and it was used after purification by dissolution in tetrahydrofuran (THF, Wako Pure Chemical Industries, Ltd.) and reprecipitation into distilled water. Other solvents and chemicals used in this study were purchased from Wako Pure Chemical Industries, Ltd.; these were all of guaranteed reagent grade and used without further purification.

2.2. Preparation of chitin butyrate

The purified chitin was acylated with a butyryl chloride in *N*,*N*-dimethylacetamide (DMAc)–LiCl solution containing triethylamine in a manner similar to that adopted in the previous studies (Kusumi, Inoue, Shirakawa, Miyashita, & Nishio, 2008; Nishio, Matsuda, Miyashita, Kimura, & Suzuki, 1997; Sugimoto et al., 2010). ^{1}H NMR data were used for the determination of a total degree of substitution (total-DS), amide-DS, ester-DS, and DD, where amide-DS and ester-DS denote the average number of butyryl substitution associated with C2-NHCOR/C2-NH_2 and C3-OH/C6-OH, respectively, per glucosamine residue of chitin and total-DS is the sum of amide-DS and ester-DS. These quantifications were conducted in the same way as that adopted in an earlier study (Sugimoto et al., 2010). Table 1 tabulates the four parameters evaluated for the three ChB products prepared in this study. In this table, the highest total-DS (3.45) may seem strange. However, it is correct because there occurred not only amidation of amine groups but also replacements for *N*-acetate with another butyryl group, which was supported by a combination of spectroscopic analyses of FT-IR and NMR (Sugimoto et al., 2010). In fact, the amide-DS was estimated to be >1 for the all ChB samples used in the present study. Eventually, DD values were determined to be 39–72%, raising noticeably from an initial value 5% for the purified chitin. Hereafter, the obtained ChB of total-DS = x and ester-DS = y is encoded as $ChB_{x(y)}$. A weight-average DP of $ChB_{3.45(1.86)}$ was determined to be 212 by gel permeation chromatography with THF as eluent (Sugimoto et al., 2010).

Table 1
Characterization of the ChB samples used in the present study.

Sample code	Total-DS	Ester-DS	Amide-DS	DD (%)	T_g (°C)	Miscibility* with PCL
$ChB_{2.34(1.19)}$	2.34	1.19	1.15	39	134	IM
$ChB_{2..93(1.76)}$	2.93	1.76	1.16	46	125	PM
$ChB_{3.45(1.86)}$	3.45	1.86	1.59	72	97	M

* Abbreviations M, PM, and IM indicate miscible, partially miscible, and immiscible, respectively.

2.3. Blend preparation

ChB/PCL blends in 50/50 in a weight percent ratio were prepared in film form from mixed polymer solutions by solvent evaporation with *N*,*N*-Dimethylformamide (DMF) as a common solvent. 3-wt% solutions of ChB and PCL were prepared separately and mixed with each other in 50/50 in a weight percent ratio. The as-cast samples were washed with distilled water and dried at 40 °C under vacuum for more than 3 days. Subsequently, film sheets were prepared by using a SA-302 hot-pressing apparatus (Tester Sangyo Co., Ltd.). For the molding, (i) the as-cast samples were first sandwiched between two Teflon release sheets with a stainless spacer, 0.1-mm thick; (ii) the set was inserted between two stainless plate and pressure was applied at 180 °C to each molten blend gradually to reach 5 MPa in 3 min; after that, it was increased quickly to 15 MPa, and this application was maintained for 30 s; (iii) as soon as the pressure was released, the sample was another compressing apparatus and quickly cold-pressed at 25 °C and 15 MPa for 2 min. After being released again from the compressed state, the molded polymer sheet was finally conditioned at 23 °C and 50% RH for 2 weeks.

2.4. Measurements

DSC was performed by using a Hitachi High-Tech Science Corporation DSC6200/EXSTAR6000 apparatus. The measurements were carried out on 7-mg film samples under a nitrogen atmosphere after calibrating the temperature readings with an indium standard. The samples were first heated from −150 °C to 200 °C at a scanning rate of 20 °C/min (first heating scan) and then immediately quenched to −150 °C at a rate of ∼80 °C/min. The second heating scans were run from −150 °C to 200 °C at a scanning rate of 20 °C/min. For estimation of the glass transition temperature (T_g) of each sample, the midpoint of the discontinuity in heat flow was recorded using the second heating scan. The melting temperature (T_m) and the enthalpy of fusion (ΔH_f) were determined from the maximum and the area of the melting endotherm, respectively, in the first heating scan.

Wide-angle X-ray diffraction (WAXD) measurements were made for the film specimens with a Rigaku Ultima-IV diffractometer at 20 °C in a reflection mode. Nickel-filtered CuKα radiation was

used at 40 kV and 40 mA. The diffraction intensity profiles were collected in the range of $2\theta = 10–30^{\circ}$.

Solid-state NMR experiments were carried out at 20 °C with a Varian Unity INOVA 400 WB NMR apparatus operated at a ^{13}C frequency of 100.6 MHz, using the aforementioned film specimens of PCL and blend samples. The magic angle spinning rate was 15 kHz. ^{13}C CP/MAS spectra were measured with a contact time of 7.0 ms. A 90° pulse width of 2.8 μs was used with 2048 FID signal accumulations. In quantification of proton spin-lattice relaxation times ($T_1{}^H$), a contact time of 1 ms was used and a proton spin-locking time τ ranged from 0.1 to 1 s. A total of 1024 scans were accumulated for the $T_1{}^H$ measurement.

For tensile tests, specimens were cut from the sheet of blends to dumbbell-type test pieces (JIS K6251: length and width of the narrow portion, 12 mm and 2 mm, respectively) with a thickness of 0.1 mm. Tensile behavior was examined for these specimens at 23 °C by using a Shimadzu Autograph AGS-5kNG. The strain rate and span length were 0.75 mm/min and 15 mm, respectively. Three specimens of each blend sample were employed for the measurement and the averaged data were adopted.

Contact angle was measured with an optical contact angle meter (Kyowa Interface Science Co., Ltd., Drop Master 500) by $\theta/2$ method at 25 °C. Distilled water (1.5 μL) was dropped carefully onto the surface of the blend sheets. An average value was obtained by measuring the same sample at five different positions.

The surface morphology of the specimens was observed using a field emission scanning electron microscopy (FE-SEM) (S-4800, Hitachi High-Technologies Corporation) at 1.5 kV. The samples were coated with Pt by sputtering.

2.5. Alkaline treatment

Three 1-squre-cm specimens cut from the above thermally molded sheet was placed in a test tube containing 2-M NaOH aqueous solution. The alkaline hydrolysis was carried out at 37 °C for 48 h in a rotary shaker (100 rpm). After that, the specimens were taken out and washed thoroughly with ethanol, then dried in vacuo at 23 °C until their weights reached constancy. Those specimens of the respective ChB/PCL blends were evaluated for the weight loss in the alkaline hydrolysis. The surface composition of the specimens was estimated by using a Shimadzu IR Prestige-21 equipped with a Shimadzu AIM-8800 infrared microscope combined with an attenuated total reflection (ATR) prism made of Ge.

2.6. Cytocompatibility test

L929 fibroblast cells (European Collection of Cell Cultures) derived from mouse were cultured on the specimens of the original ChB and PCL and their blends before and after alkaline hydrolysis, in Eagle's minimal essential medium (Eagle's MEM, Nissui Pharmaceutical Co.) at 37 °C in a humidified atmosphere of 95% air and 5% CO_2. 1000 mL of the Eagle's MEM included 15 mL of supplemental mixture solution containing 10.0-wt% fetal bovine serum (FBS, Sigma Co.), 3-wt% L-glutamine, and 8-wt% sodium hydrogen carbonate. Prior to the cell adhesion studies, all films were sterilized by immersing in Eagle's MEM containing Kanamycin for 5 h. The L929 cells were seeded onto the sterilized specimens at a population density of 1.0×10^5 cells/mL for the cell-adhesion investigations. After cultivation, the films were gently rinsed twice with phosphate buffered saline to remove cells weakly adhered on the surface. Subsequently, the specimens were soaked in the 2.5 wt% glutaraldehyde solution at 4 °C for 12 h, and then dehydrated with 10-min exposures to successive 30, 50, 70, 90, and 100% concentrations of ethanol.

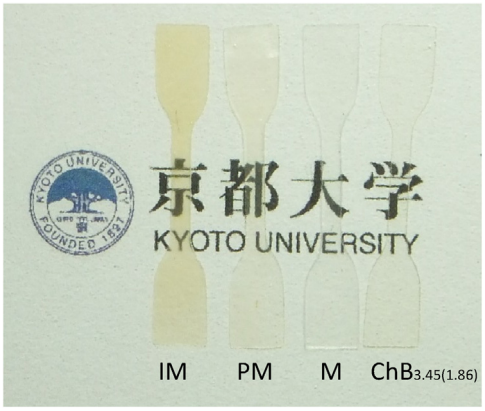

Fig. 1. Visual appearance of the hot-press molded (180 °C) films of $ChB_{3.45(1.86)}$ and IM, PM, and M blends (ChB/PCL = 50/50 in weight).

3. Results and discussion

3.1. Sample overview

Table 1 lists the characterization data for the ChB samples used in the present study as well as their miscibility with PCL. Blend pairs of these ChB samples were classified into immiscible (IM), partially miscible (PM), and miscible (M) ones in their amorphous states by differential scanning calorimetry (DSC). The thermograms of the second heating scan were shown in Fig. S2. The immiscibility was judged from an observation of no significant shift in glass transition temperature (T_g) for both components. For M blends, a single T_g was detected and varied between the T_g values of the two constituent polymers, depending on the blend compositions. PM blends gave rise to just a slight shift in the T_g of the ChB component but an elevation in the PCL T_g. The T_g shift for PM and M was prominent only at compositions rich in ChB, as has been experienced before, (Sugimoto et al., 2010) while 50/50 blend samples were used in the present study.

Fig. 1 demonstrates the visual appearances for the film specimens of $ChB_{3.45(1.86)}$ and 50/50 (in weight) blends in different miscibility states. For preparing the specimens, solution cast blend films were hot-pressed at 180 °C and cut into dumbbell-type test pieces for tensile measurements. The ~0.1-mm-thick film specimens were visually homogeneous and exhibited transparency. The highest transmittance was observed for the $ChB_{3.45(1.86)}$ film (78% at 550 nm). The transparency of ChB was diminished by blending PCL, which usually gives white opaque thermally-molded sheets due to coexistence of macroscopic crystalline texture and amorphous domain. The transmittance at 550 nm decreased in the order of miscibility and was estimated to be 52, 39, and 24% for the M, PM, and IM blends, respectively. This result may reflect a heterogeneity in the scale of more than ~100 nm depending on the degree of miscibility, but it is difficult to simply explain the tendency because the visual appearance would be varied not only by a mixing scale of the blend components but also with the difference of the PCL crystalline organization. The yellow-brownish color observed for the IM blend might be derived from relatively less thermoplasticity of the ChB component ($ChB_{2.34(1.19)}$).

3.2. Crystallinity

For the miscibility judgment by estimating T_g of the blends, we conducted DSC analysis (Fig. S2) in the second heating scan after rapid cooling (~80 °C/min) from a molten state. On the other hand, the film specimens provided for the tensile testing preserved another thermal history (stored at 23 °C for 2 weeks after

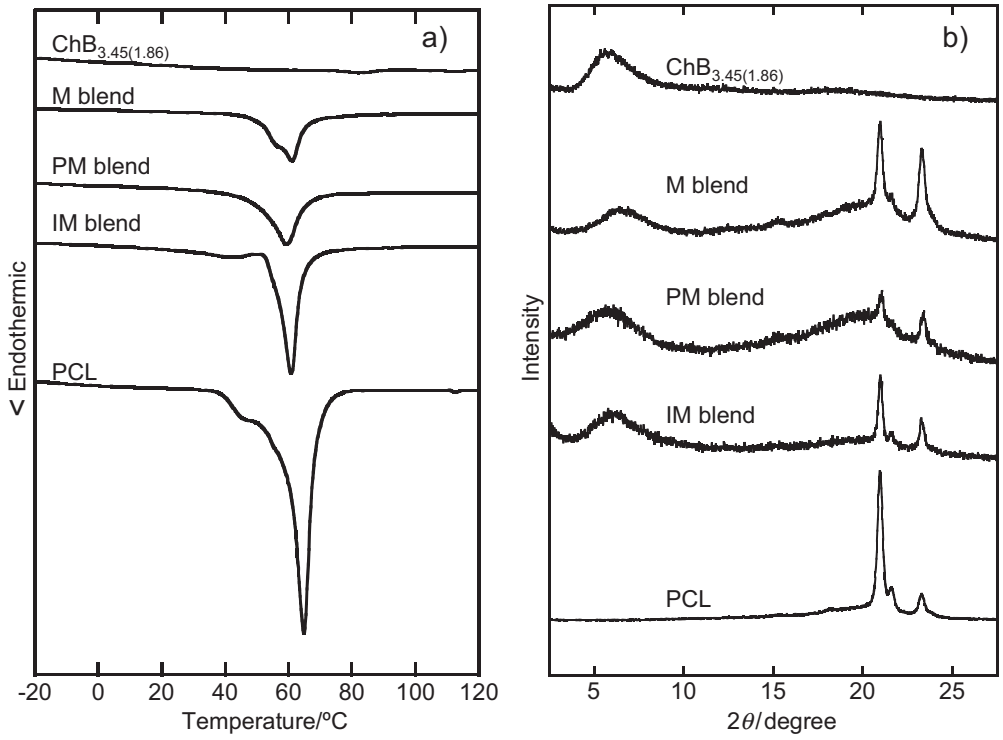

Fig. 2. (a) DSC thermograms (first heating scan) and (b) WAXD profiles of $ChB_{3.45(1.86)}$, IM, PM, and M blends (ChB/PCL = 50/50 in weight), and PCL, measured for their film specimens stored at 23 °C for 2 weeks after thermal molding.

thermal molding). All DSC thermograms (Fig. 2a) in the first heating scan for the specimens show a melting endotherm and no cold-crystallization exotherm, indicating sufficient development of PCL crystal in the storage period.

Using the DSC thermograms illustrated in Fig. 2a, the crystallinity index X_c can be calculated per net weight of PCL component, from the following equation:

$$X_c = \frac{\Delta H_m}{(0.5\Delta H_m^o)} \quad (1)$$

where $\Delta H_m^\circ = 136$ J/g (Khambatta, Warner, Russell, & Stein, 1976) is the heat of fusion of 100% crystalline PCL and 0.5 is the weight fraction of the PCL component. The result is listed in Table 2. As shown there, both the T_m and X_c of the blends decreased with increasing degree of miscibility. In general, the decreasing action can be primarily ascribed to a morphological effect such as lowering of the size of crystallites for all the blend pairs. In addition, for the M and PM blend systems, there may be a contribution of the so-called thermodynamic diluent effect (Scott, 1949) by the acyl chitin, even though quantitative analysis of isothermal crystallization behavior is necessary to discuss in detail. However, the possible highest diluent effect for the M blend probably gave rise to the largest range of reduction for the T_m and X_c.

Fig. 2b displays WAXD profiles obtained at 23 °C for the film specimens with the identical thermal history (stored at 23 °C for 2 weeks after thermal molding). For the unblended PCL sample, three distinctive diffraction peaks observed at $2\theta = 21.4°$, 22.0°, and 23.7°, which are indexed as (1 1 0), (1 1 1), and (2 0 0), respectively (Chatani, Okita, Tadokoro, & Yamashita, 1970). The average crystallite size of the PCL component was estimated from the full-width half maximum (FWHM) of a WAXD peak at $2\theta = 21.4°$ derived from the (1 1 0) plane using the Scherrer's formula:

$$D = \frac{0.94\lambda}{(\beta\cos\theta)} \quad (2)$$

where λ (= 0.154 nm) is the wavelength of the X-ray used, β is the FWHM of the peak and $\cos\theta$ is the Bragg diffraction angle. The results of the calculation were tabulated in Table 2. As seen in this table, the D decreased by blending the ChB having more or less miscibility with PCL, and the value was specifically small for the PM blend. This decrease indicates an overall reduction in size and/or regularity of the formed PCL crystal for these blends. The difference in dimension and dispersion of the PCL crystallites was also suggested by a contrast between spherulitic morphologies of M and PM blends (see Supporting information, Fig. S3). Eventually, for the PM blend, the PCL crystallite with small correlation length, in other words, the microcrystallite of PCL was well dispersed in the molded blend films.

Table 2
Thermal and crystallographic property of ChB/PCL blends (50/50 in weight) and PCL, measured for their film specimens stored at 23 °C for 2 weeks after thermal molding.

Sample code	T_m (°C)	ΔH_m (J/g)	$X_{c(PCL)}$ (%)	D (nm)
M blend	58	20.6	30.3	25.4
PM blend	59	23.4	34.5	11.6
IM blend	61	32.2	47.4	33.7
PCL	65	92.5	68.0	29.4

3.3. Quantification of domain size by T_1^H measurement

In order to further elucidate the microscopic morphological situation in several tens of nanometers, we tried to evaluate a mixing scale of the blend components using solid-state NMR. As is well established, ^{1}H spin-lattice relaxation time ($T_1{}^H$) measurements in solid-state ^{13}C NMR spectroscopy provide information about some microphase structure of polymers in a scale of a few tens of nanometers. ^{13}C CP/MAS spectra and the peak assignments are shown in Fig. 3. The relaxation process was monitored for the peak intensities of C3/C4/C5 pyranose carbons and C4′ methyl carbon of the ChB component and for those of C3″/C4″ and C5″ methylene

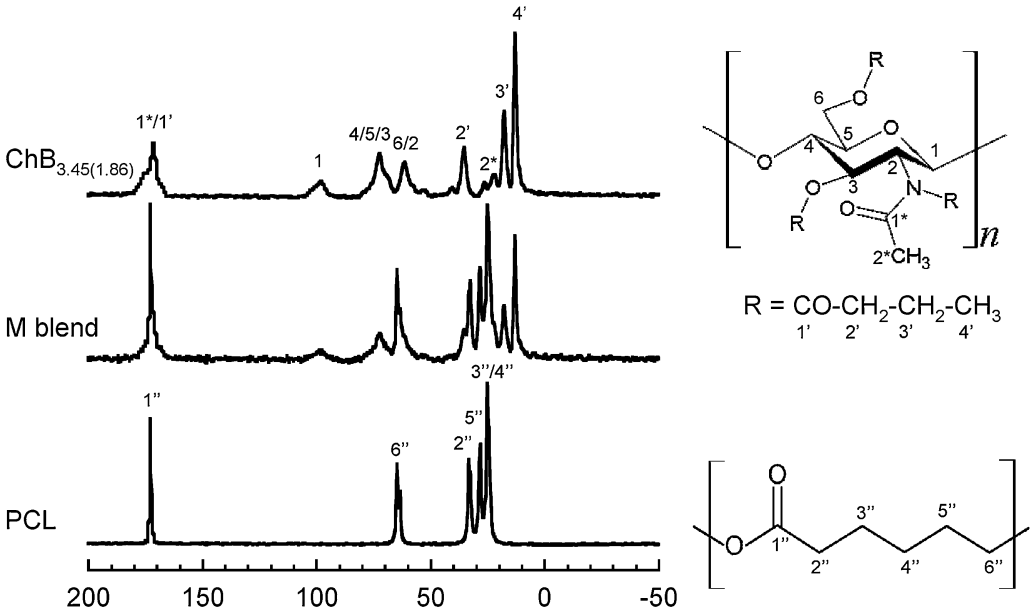

Fig. 3. Solid-state ^{13}C CP/MAS NMR spectra of $ChB_{3.45(1.86)}$, M blend, and PCL.

Table 3
Values of $T_1{}^H$/s for $ChB_{2.93(1.76)}$, ChB/PCL (50/50 in weight) blends, and PCL.

Sample code	ChB		PCL		L (nm)
	Pyranose C4/C5/C3 (74.7 ppm)	C4′ (13.2 ppm)	C3″/C4″ (24.7 ppm)	C5″ (28.2 ppm)	
$ChB_{2.93(1.76)}$	1.41	1.37	–	–	–
M blend	1.07	1.12	1.13	1.11	43.9–52.1
PM blend	1.06	1.00	1.03	1.04	42.4–50.4
IM blend	1.35	1.40	0.96	0.96	–
PCL	–	–	0.90	0.98	–

carbons of the PCL component. T_1^H values can be obtained practically by fitting the carbon resonance intensity to the following exponential equation

$$M(\tau) = M_0\left(1 - 2\exp\left(\frac{-\tau}{T_1^H}\right)\right) \quad (3)$$

where $M(\tau)$ is the magnetization intensity observed as a function of the spin-locking time τ and the initial intensity is given by $M(0) = -M_0$. As a general rule, if two polymer components are in a homogeneous mixing state on the scale over which ^{1}H spin diffusion can take place in a time T_1^H, the T_1^H values for different protons belonging to the respective components may be equalized to each other. The result of the T_1^H measurements is summarized in Table 3. In the M and PM blends, the T_1^H of ChB diminishes appreciably while that of PCL rather rises, so that these values almost coincide with each other. Such an attunement was not observed for the IM blend. It is therefore reasonable to assume that the two constituent polymers in the M and PM blends are coexistent in a range where the mutual ^{1}H-spin diffusion is permitted over a period of the respective homogenized T_1^H, e.g., 1.00–1.13 s.

An effective path length L of the spin diffusion in a time T_1^H is given by the following equation (McBrierty & Douglass, 1981):

$$L \approx \left(6DT_1^H\right)^{0.5} \quad (4)$$

where D is the diffusion coefficient, taken to be $4–6 \times 10^{-16}$ m^2/s for PCL (Huang & Yang, 2005). Substitution of the T_1^H data obtained above into this equation leads to the assessment of L as an upper limit of the heterogeneous domain size in the relevant blends. By simple application of this relation with the T_1^H data, the diffusion path lengths are calculated as L = 43.9–52.1 and 42.4–50.4 nm for the M and PM blends, respectively. Thus, these blends were found to be actually homogeneous with an upper limit of ca. 50 nm in the T_1^H measurements. The homogeneity of the amorphous domain for the M blend has already been ensured being on a couple of tens nanometers by the T_g detection with DSC. In the PM blend, it follows that the homogeneity lies on a certain scale between 20 and 50 nm.

3.4. Tensile mechanical properties

Fig. 4 shows the stress–strain curves obtained for the specimens of the $ChB_{3.45(1.86)}$, PCL, and 50/50 blends of ChB/PCL at 23 °C. The numerical values determined by the tensile test were listed in Table 4. Basically, original mechanical properties of the blend

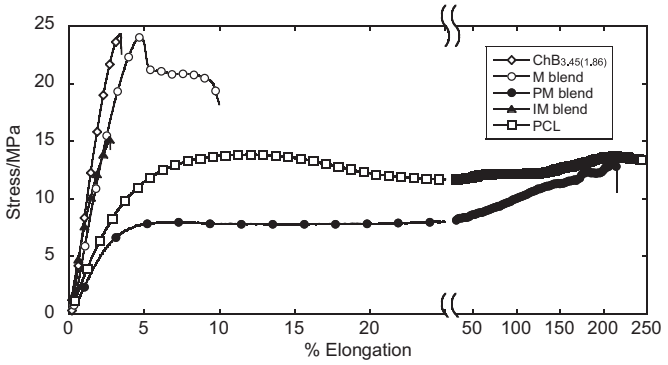

Fig. 4. Stress–strain curves for $ChB_{3.45(1.86)}$, IM, PM, and M blends (ChB/PCL = 50/50 in weight), and PCL.

Table 4
Tensile mechanical properties of $ChB_{3.45(1.86)}$, ChB/PCL (50/50 in weight) blends in various miscibility states, and PCL, measured for their film specimens stored at 23 °C for 2 weeks after thermal molding. Numbers shown in parentheses are standard deviations.

Sample code	Young's modulus (MPa)	Yield stress (MPa)	Elongation at rupture (%)	Stress at rapture (MPa)
$ChB_{3.45(1.86)}$	631 (20)	–	3.5 (0.3)	24.3 (1.6)
M blend	445 (16)	16.9 (0.2)	28.1 (3.0)	15.0 (1.8)
PM blend	170 (3)	7.9 (0.1)	215 (26)	12.7 (1.5)
IM blend	425 (8)	–	2.7 (0.3)	15.2 (0.4)
PCL	285 (16)	13.9 (0.7)	>333	>13.9

components are in contrast with each other: stiff and brittle for ChB of relatively high strength and modulus; flexible and ductile for PCL with low modulus. The results revealed that there was essentially no improvement for the IM blend pair due to poor interfacial adhesion between the blend components. On the other hand, for the M and PM blends, we found a remediation of the brittleness and an increase in ductility of ChB by blending PCL. However, the tensile properties of these blend films were not simple arithmetic average of the original materials, but were strikingly influenced by the degree of miscibility. Namely, the elongation at rapture for the PM blend films was estimated to be >200%, which was extraordinarily larger than that for the M blend. The PM blend also exhibited a lower Young's modulus in comparison with the other blends.

Such contrasting results for the M and PM blends can be explained as follows. For the M blend system, an interface region can be taken to be absent on a scale of larger than 20 nm. However, because of a possible interaction between the chitinous and PCL molecules, a restriction of the deformation of the PCL molecules might give rise to a moderate improvement of the ductility, even if the T_g of the blend is lower than the test temperature. On the other hand, for the PM blend, there might be a balance in crystallite dimension and domain size, favorable for the improvement of ductility: (1) the ductility might be improved by the miniaturization of the PCL crystallite as an effective physical cross-linker and/or nanofiller and (2) the scale of mixing between 20 and 50 nm might bring about appropriate interaction between the ChB and PCL molecules so as not to interfere with the flexibility of PCL but to provide a domain as if acting as cross-linking.

Accordingly, we found that a striking difference in the mechanical property for the ChB/PCL blends was produced by the variation of the degree of miscibility based on the alteration of DS, where the PM blend exhibited the highest ductility.

3.5. Alkaline treatment and cytocompatibility

We examined an alkaline treatment (2 M NaOH at 37 °C) for the thermally molded films of the ChB/PCL blends, expecting the improvement of the surface hydrophilicity and accessibility by cells. When 48 h passed, even though the IM blend film became too brittle to remain the initial shape after the alkaline treatment, the other two blends maintained their original film forms. The weight loss values were 0.83, 14.2, and 76.0 wt% for the M, PM, and IM blends respectively. The M, PM, and IM blends before the alkaline treatment showed contact angle values of $88.0 \pm 6°$, $85.0 \pm 2.7°$, and $88.5 \pm 1.5°$ for distilled water, respectively. After the alkaline treatment, a decrease in the contact angle values was observed for the M and PM blends ($74.7 \pm 0.9°$ and $67.2 \pm 1.4°$, respectively), which indicates an improvement of surface hydrophillicity for these samples by the alkaline treatment. However, it was difficult to obtain the data for the IM after the alkaline hydrolysis due to its brittleness.

To disclose what caused the weight loss and contact angle variation, the surface composition was examined by microscopic ATR-FTIR. Fig. 5 exemplifies the spectra. In ATR spectroscopy, the penetration depth (d_p) is defined as the distance from the germanium ATR prism-sample interface where the intensity of the evanescent wave decays to $1/e$ (approximately 37%) of its original value. The d_p is expressed by

$$d_p = \frac{\lambda/2\pi n_1}{\left(\sin^2\theta - \left(n_2/n_1\right)^2\right)^{0.5}} \quad (5)$$

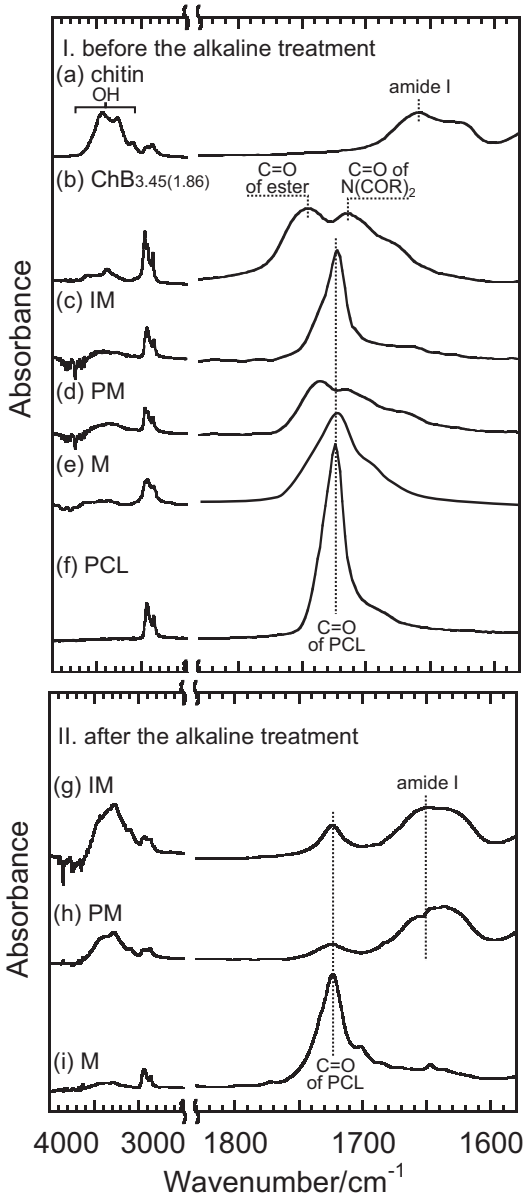

Fig. 5. Microscopic ATR-FTIR spectra of film specimens (I) before and (II) after the alkaline hydrolysis (2-M NaOH at 37 °C for 48 h): (a) chitin, (b) $ChB_{3.45(1.86)}$, blends of (c) IM, (d) PM, and (e) M, and (f) PCL before the alkaline treatment; (g) IM, (h) PM, and (i) M blends after the alkaline treatment. ChB/PCL ratio of the original blend materials was 50/50 in weight.

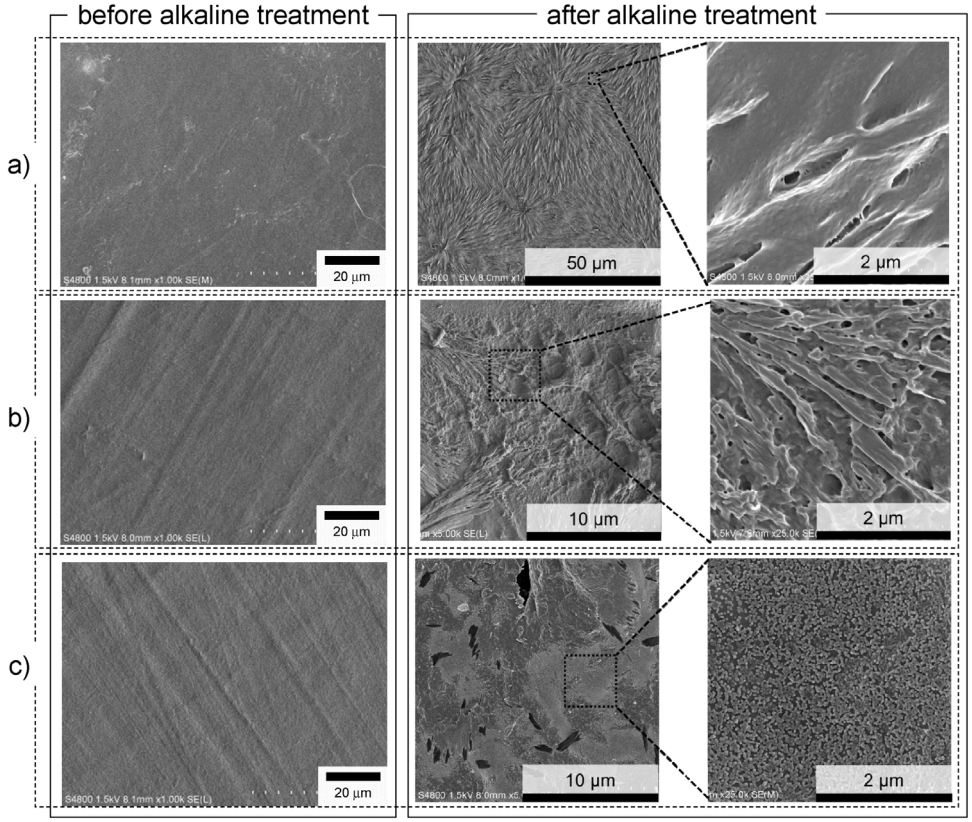

Fig. 6. FE-SEM images of (a) M, (b) PM, and (c) IM blends (the original ChB/PCL weight ratio, 50/50) before and after the alkaline treatment.

where θ is the angle of incidence of the light beam, λ the wavelength of infrared-light absorption, n_1 the refractive index of the ATR prism used, and n_2 the refractive index of the sample. In the present study, the d_p value can be estimated as ca. 0.17–0.41 μm for the spectra (4000–1600 cm^{-1}), if we substitute $\theta = 45^\circ$ and $n_1 = 4$ (for Ge), with a tentative value of $n_2 = 1.5$. The actual sampling depth d_s is defined by the full absorption of the evanescent wave and known to be about $3d_p$. Therefore, the spectra illustrated in Fig. 5 reveal the depth-dependent distribution of the chemical compositions ranging from 0.5 to 1.2 μm in depth for the film samples.

In the spectra of the original materials (Fig. 5(I)), specific absorption bands were present in the spectral region associated with OH (3100–3700 cm^{-1}) and amide I (1655 cm^{-1}) for chitin (a) and with ester C=O (1720 cm^{-1}) for PCL (f), respectively. For $ChB_{3.45(1.86)}$ (b), remarkable developments in absorption were observed in 1740 cm^{-1} and 1710 cm^{-1}, being assigned to the introduced C=O of ester and $N(COR)_2$ moieties, respectively (Sugimoto et al., 2010), although the former band shifted to the higher wavenumber in comparison with the ester C=O band of PCL. The smaller wavenumber of the signal of C=O for PCL is likely due to the crystallinity. In common with the observation for the highly substituted ChB of total-DS > ~3 in our previous study (Sugimoto et al., 2010), we found a suppression in the amide I band, as manifested for the spectrum (b) of $ChB_{3.45(1.86)}$. Meanwhile, the spectra (c) and (e) of the IM and M blends, respectively, before the alkaline hydrolysis appeared similar to that of PCL (f), suggesting the surface segregation of the PCL component for the hot-press molded films.

In Fig. 5(II), we also demonstrate the spectra (g)–(i) for the blend films after the alkaline hydrolysis. Those three spectra can be classified into two groups according to the shape. Namely, in the spectra of the IM (g) and PM (h) blends after the hydrolysis, we can see the strong bands ascribable to chitinous OH (3100–3700 cm^{-1}) and amide I (1655 cm^{-1}) and a moderate one at 1720 cm^{-1} of ester C=O. The ester C=O band was probably originated with the PCL component because the band location is similar to the one of the plain polyester (f). Therefore, for the surface region of these two alkaline-treated blend films up to ~1.2 μm in depth, we can assume a formation of chitin by an almost complete removal of the butyryl moiety of ChB and an appreciable elution of the PCL component. These observations are consistent with the noticeable weight loss by the alkaline hydrolysis, as has been mentioned above. On the other hand, the spectrum for the alkaline-treated film of the M blend (i) seems like that of the original blend (e). Taking into consideration the much less weight loss (0.83 wt%) by the alkaline treatment for the M blend, there was just a slight effect on the chemical composition for the film specimen by the alkaline treatment.

Fig. 6 displays FE-SEM images of the blend films, which were acquired before and after the alkaline hydrolysis over a period of 48 h. The as-prepared films showed an essentially smooth surface with lines originating from the surface shape of Teflon substrates for thermal molding. On the other hand, the surface morphology of the alkaline-treated films was basically rough and exhibited three different geometries depending on the miscibility. Namely, we can see several radial textures on the surface of the M blend film (a), which might be the spherulitic textures exposed by an etching effect after the removal of the chitinous and amorphous PCL components by the alkaline treatment. This observation is consistent with the microscopic ATR-FTIR data, where the PCL component is mainly present on the surface. For the PM blend (b), the surface after alkaline treatment exhibited relatively random asperity on larger scale. By comparing enlarged images of the M and PM blends, a remarkable eluviation was observed for the latter one. According to the above ATR-FTIR data, it may be reasonable to assume that what we see is mainly composed of chitin. On the other hand, the IM blend (c) presented a further random and inhomogeneous surface with aggregation of granular particles, as shown in the enlarged one.

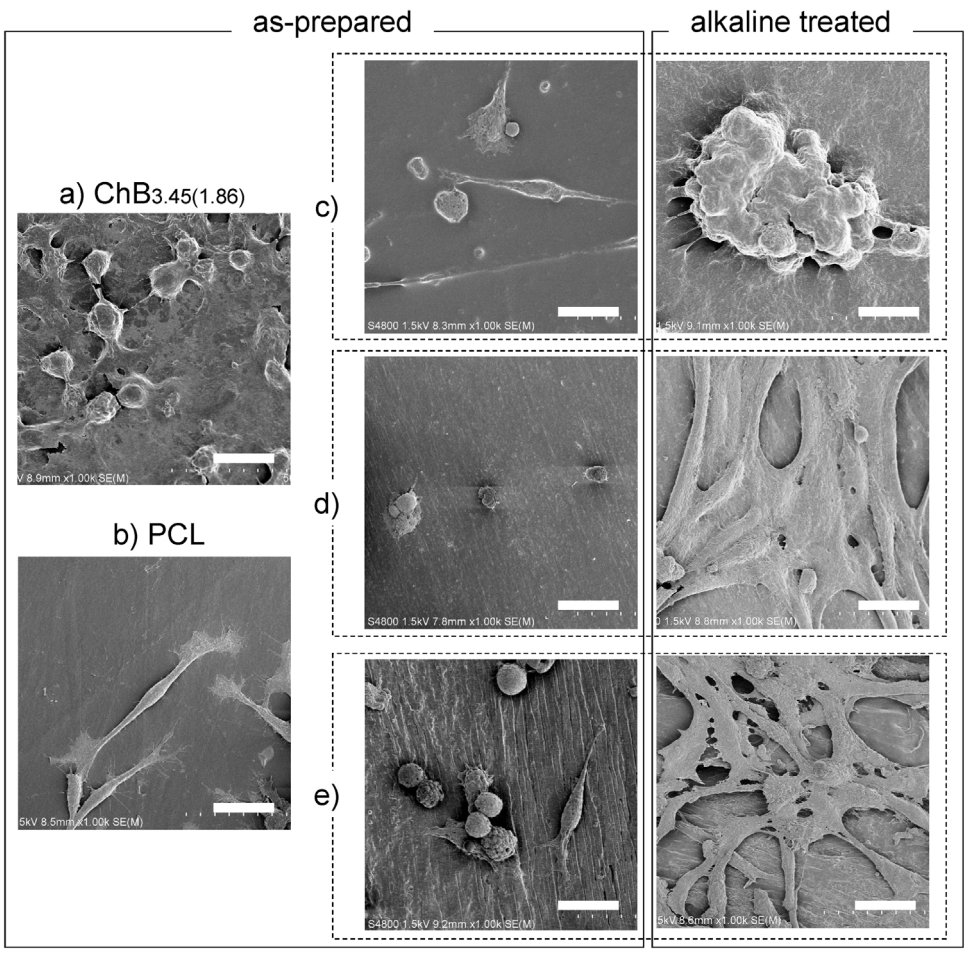

Fig. 7. FE-SEM images of cell growth on the films of (a) $ChB_{3.45(1.86)}$, (b) PCL, and (c) M, (d) PM, and (e) IM blends (the original ChB/PCL weight ratio for the blends, 50/50). The images of the blend films (c)–(e) include the ones after the alkaline treatment. Scale bars denote 20 μm.

To evaluate cell adhesion and proliferation, L929 fibroblast cells were seeded on the blend films. In Fig. 7, FE-SEM micrographs demonstrate the morphologies of cells that were cultured for 48 h on the as-pressed films of $ChB_{3.45(1.86)}$, PCL, and the blends as well as the alkaline-treated ones of the blends. On the films without the alkaline treatment, some of the cells were spread and flattened, but many were still round, and this indicated an absence of strong cell-films interaction. On the other hand, for the alkaline-treated blend films except the M blend, the adherence of cells to the surfaces was densely distributed in comparison with those without the alkaline treatment. This observation indicates the evidence of the anchoring ligands reaching out to help support the cells on the film surface of the alkaline treated PM and IM blend films.

Resultingly, we consider that the high porosity of these two alkaline-treated films provides more structural space for cell accommodation and makes the exchange of nutrient and metabolic waste between the scaffold and environment more efficient. In addition, the surface exposure of the chitinous component for the PM and IM blend films alkaline-treated, confirmed by the ATR-FTIR analysis, not only improve the hydrophilicity of the films but also provide the necessary active sites through which other biocompatible components such as proteins, polysaccharides, cell growth factors, or peptides can be further immobilized.

From this evidence, the cell adhesion on the thermoplastic ChB/PCL blend films can be improved via alkaline-hydrolysis and the important factor was the degree of miscibility for the original blend films in order to promote cell attachment, cell proliferation, and proper cell spreading. In the present study, it can be concluded that the PM blend is the most appropriate scaffold from the balance of the specific ductile nature and the cytocompatibility after the alkaline treatment.

4. Conclusions

In the present study, thermoplastic transparent films of ChB/PCL blends were successfully fabricated by hot-press molding. Even though no modification effect in mechanical property was observed for IM blend, we found a remediation of the brittleness and an increase in ductility of ChB for the M and PM blend with PCL. In particular, the PM blend exhibited the highest ductility, which may be ascribable to a balance in the dimension and dispersion of the PCL microcrystallites and the domain size of the blend components. Subsequent alkaline treatment gave rise to the high porosity and the surface exposure of chitinous component for the PM and IM blend films. Cell culture imaging confirmed that the PM and IM blend after the alkaline treatment were the best in promoting the cell attachment and proliferation. Taking into consideration the ductility and cytocompatibility, the PM blend was a good candidate for use as thermoplastic scaffolding materials capable of wide application.

Acknowledgments

The authors wish to acknowledge Professor Takashi Nishino of Kobe University for providing the procedure of cytocompatibility test. This work was supported by Adaptable and Seamless

Technology Transfer Program though Target-driven R&D (A-STEP) (No. AS231Z01846F to Y.T.), provided by Japan Science and Technology Agency (JST).

Appendix A. Supplementary data

Supplementary material related to this article can be found, in the online version, at http://dx.doi.org/10.1016/j.carbpol.2014.08.028.

References

Chatani, Y., Okita, Y., Tadokoro, H., & Yamashita, Y. (1970). Structural studies of polyesters. III. Crystal structure of poly-ε-caprolactone. *Polymer Journal*, *1*, 555–562.

Chen, B., Sun, K., & Ren, T. (2005). Mechanical and viscoelastic properties of chitin fiber reinforced poly(ε-caprolactone). *European Polymer Journal*, *41*, 453–457.

Draczynski, Z., Bogun, M., Mikolajczyk, T., Szparaga, G., & Krol, P. (2013). The influence of forming conditions on the properties of the fibers made of chitin butyryl-acetic copolyester for medical applications. *Journal of Polymer Science*, *127*, 3569–3577.

Dubas, S. T., Kittitheeranun, P., Rangkupan, R., Sanchavanakit, N., & Potiyaraj, P. (2009). Coating of polyelectrolyte multilayer thin films on nanofibrous scaffolds to improve cell Adhesion. *Journal of Applied Polymer Science*, *114*, 1574–1579.

Hackman, R. (1954). Studies on chitin. 1. Enzymatic degradation of chitin and chitin esters. *Australian Journal of Biological Sciences*, *7*, 168–178.

He, L., Shi, Y., Han, Q., Zuo, Q., Ramakrishna, S., Xue, W., et al. (2012). Surface modification of electrospun nanofibrous scaffolds via polysaccharide–protein assembly multilayer for neurite outgrowth. *Journal of Materials Chemistry*, *22*, 13187–13196.

Honma, T., Senda, T., & Inoue, Y. (2003). Thermal properties and crystallization behaviour of blends of poly(ε-caprolactone) with chitin and chitosan. *Polymer International*, *52*, 1839–1846.

Huang, J. M., & Yang, S. J. (2005). Studying the miscibility and thermal behavior of polybenzoxazine/poly(3-caprolactone) blends using DSC, DMA, and solid state ^{13}C NMR spectroscopy. *Polymer*, *46*, 8068–8078.

Jayakumar, R., Prabaharan, M., Nair, S. V., & Tamura, H. (2010). Novel chitin and chitosan nanofibers in biomedical applications. *Biotechnology Advances*, *28*, 142–150.

Jeong, S. I., Jun, I. D., Choi, M. J., Nho, Y. C., Lee, Y. M., & Shin, H. (2008). Development of electroactive and elastic nanofibers that contain polyaniline and poly(L-lactide-*co*-ε-caprolactone) for the control of cell adhesion. *Macromolecular Bioscience*, *8*, 627–637.

Khambatta, F. B., Warner, F., Russell, T., & Stein, R. S. (1976). Small-angle X-ray and light-scattering studies of morphology of blends of poly(ε-caprolactone) with poly(vinyl chloride). *Journal of Polymer Science B: Polymer Physics*, *14*, 1391–1424.

Khor, E., & Lim, L. Y. (2003). Implantable applications of chitin and chitosan. *Biomaterials*, *24*, 2339–2349.

Kusumi, R., Inoue, Y., Shirakawa, M., Miyashita, Y., & Nishio, Y. (2008). Cellulose alkyl ester/poly(ε-caprolactone) blends: Characterization of miscibility and crystallization behaviour. *Cellulose*, *15*, 1–16.

McBrierty, V. J., & Douglass, D. C. (1981). Recent advances in the NMR of solid polymers. *Journal of Polymer Science D: Macromolecular Reviews*, *16*, 295–366.

Muzzarelli, R. A. A. (2009). Chitins and chitosans for the repair of wounded skin, nerve, cartilage and bone. *Carbohydrate Polymers*, *76*, 167–182.

Muzzarelli, R. A. A., Guerrieri, M., Goteri, G., Muzzarelli, C., Armeni, T., Ghiselli, T., et al. (2005). The biocompatibility of dibutyryl chitin, in the context of wound dressings. *Biomaterials*, *26*, 5844–5854.

Nishio, Y., Matsuda, K., Miyashita, Y., Kimura, N., & Suzuki, H. (1997). Blends of poly(ε-caprolactone) with cellulose alkyl esters: Effect of the alkyl side-chain length and degree of substitution on miscibility. *Cellulose*, *4*, 131–145.

Pant, H. R., Kim, H. J., Bhatt, L. R., Joshi, M. K., Kim, E. K., Kim, J. I., et al. (2013). Chitin butyrate coated electrospun nylon-6 fibers for biomedical applications. *Applied Surface Science*, *285*, 538–544.

Prabhakaran, M. P., Venugopal, J. R., Chyan, T. T., Hai, L. B., Chan, C. K., Lim, A. Y., et al. (2008). Electrospun biocomposite nanofibrous scaffolds for neural tissue engineering. *Tissue Engineering A*, *14*, 1787–1797.

Sannan, T., Kurita, K., Ogura, K., & Iwakura, Y. (1978). Studies on chitin. 7. IR spectroscopic determination of degree of deacetylation. *Polymer*, *19*, 458–459.

Sarasam, A., & Madihally, S. V. (2005). Characterization of chitosan–polycaprolactone blends for tissue engineering applications. *Biomaterials*, *26*, 5500–5508.

Scott, R. L. (1949). The thermodynamics of high polymer solutions. V. Phase equilibria in the ternary system: Polymer 1–polymer 2–solvent. *Journal of Chemical Physics*, *17*, 279–284.

Senda, T., He, Y., & Inoue, Y. (2002). Biodegradable blends of poly(ε-caprolactone) with alpha-chitin and chitosan: Specific interactions, thermal properties and crystallization behavior. *Polymer International*, *51*, 33–39.

Sugimoto, M., Kawahara, M., Teramoto, Y., & Nishio, Y. (2010). Synthesis of acyl chitin derivatives and miscibility characterization of their blends with poly(ε-caprolactone). *Carbohydrate Polymers*, *79*, 948–954.

Wan, Y., Wu, H., Cao, X., & Dalai, S. (2008). Compressive mechanical properties and biodegradability of porous poly(caprolactone)/chitosan scaffolds. *Polymer Degradation and Stability*, *93*, 1736–1741.

Zhu, Y., Gao, C., Liu, X., & Shen, J. (2002). Surface modification of polycaprolactone membrane via aminolysis and biomacromolecule immobilization for promoting cytocompatibility of human endothelial cells. *Biomacromolecules*, *3*, 1312–1319.